Selective activation of STAT5 unveils its role in stem cell self-renewal in normal and leukemic hematopoiesis

Yuko Kato,[1] Atsushi Iwama,[1,6] Yuko Tadokoro,[1] Kazuya Shimoda,[4] Mayu Minoguchi,[1,7] Shizuo Akira,[5] Minoru Tanaka,[3] Atsushi Miyajima,[3] Toshio Kitamura,[2] and Hiromitsu Nakauchi[1]

[1]Laboratory of Stem Cell Therapy, Center for Experimental Medicine, and [2]Divisions of Cellular Therapy and Hematopoietic Factors, Institute of Medical Science, University of Tokyo, Tokyo 108-8639, Japan
[3]Institute of Molecular and Cellular Biosciences, University of Tokyo, Tokyo 113-0032, Japan
[4]First Department of Internal Medicine, Faculty of Medicine, Kyushu University, Fukuoka 812-8582, Japan
[5]ERATO, Akira Innate Immunity Program, Japan Science and Technology Agency, Research Institute for Microbial Diseases, Osaka University, Osaka 565-0871, Japan
[6]Department of Cellular and Molecular Medicine, Graduate School of Medicine, Chiba University, Chiba 260-8670, Japan
[7]ReproCELL Inc., Tokyo 100-0011, Japan

Although the concept of a leukemic stem cell system has recently been well accepted, its nature and the underlying molecular mechanisms remain obscure. Constitutive activation of signal transducers and activators of transcription 3 (STAT3) and STAT5 is frequently detected in various hematopoietic tumors. To evaluate their role in normal and leukemic stem cells, we took advantage of constitutively active STAT mutants to activate STAT signaling selectively in hematopoietic stem cells (HSCs). Activation of STAT5 in CD34$^-$c-Kit$^+$Sca-1$^+$ lineage marker$^-$ (CD34$^-$KSL) HSCs led to a drastic expansion of multipotential progenitors and promoted HSC self-renewal ex vivo. In sharp contrast, STAT3 was demonstrated to be dispensable for the HSC maintenance in vivo, and its activation facilitated lineage commitment of HSCs in vitro. In a mouse model of myeloproliferative disease (MPD), sustained STAT5 activation in CD34$^-$KSL HSCs but not in CD34$^+$KSL multipotential progenitors induced fatal MPD, indicating that the capacity of STAT5 to promote self-renewal of hematopoietic stem cells is crucial to MPD development. Our findings collectively establish a specific role for STAT5 in self-renewal of normal as well as leukemic stem cells.

CORRESPONDENCE
Atsushi Iwama:
aiwama@faculty.chiba-u.jp
OR
Hiromitsu Nakauchi:
nakauchi@ims.u-tokyo.ac.jp

Abbreviations used: EPO, erythropoietin; HPP-CFC, high-proliferative-potential colony-forming cell; HPPC, high-proliferative-potential colony; HSC, hematopoietic stem cell; KSL, c-Kit$^+$Sca-1$^+$ lineage marker$^-$; LTR, long-term repopulating; MPD, myeloproliferative disease; nmEM, neutrophil/macrophage/erythroblast/megakaryocyte; *OSM*, *Oncostatin M*; pIpC, polyinocinic-polycytidylic acid; RU, repopulation unit; SCF, stem cell factor; TPO, thrombopoietin.

Cytokine signaling pathways are important signal mediators promoting hematopoietic cell survival, proliferation, and differentiation. The JAK–STAT pathway is recognized as a common downstream pathway from cytokine receptors and plays critical roles in transmitting a variety of biological functions by activating transcription of various target genes. STAT proteins form homo- or heterodimers upon tyrosine phosphorylation, which usually is mediated by JAKs. Dimerized STAT proteins immediately enter the nucleus and bind to specific DNA sequences in promoter regions of various genes, resulting in gene activation or repression (1). To date, seven genes encoding mammalian STAT family members (STAT 1–6) have been identified. Among them is STAT5, which is encoded by two genes, *STAT5A* and *STAT5B*, with 95% sequence identity (2).

Attempts to expand HSCs ex vivo have been made under various conditions. These attempts include manipulation of transcriptional regulators such as HoxB4 and Bmi-1 (3, 4). We and others have reported that among various cytokines, thrombopoietin (TPO) promotes the self-renewal of long-term repopulating (LTR) HSCs in vitro (5, 6). BM cells from mice deficient for c-*mpl*, the gene encoding TPO receptor, failed to compete effectively with normal cells for long-term reconstitution of the hematopoietic organs of irradiated recipients, even when transplanted in 10-fold excess (7). These findings suggest that TPO signaling is a prominent and essential physiological component of HSC regulation. TPO was first characterized as a key regulator of megakaryocyte and platelet formation. TPO binding dimerizes

The online version of this article contains supplemental material.

c-mpl, thereby activating intracellular signaling cascades, including JAK–STAT, phosphatidylinositol 3-kinase/Akt, and Ras/mitogen-activated protein kinase pathways.

STAT5A and *STAT5B* doubly disrupted mice have been generated recently. They displayed a profound defect in competitive repopulation of hematopoiesis (8, 9). The commitment of embryonic stem cells to hematopoietic cells is augmented by a STAT5-mediated signal (10). A recent study showed that persistent activation of STAT5A in human cord blood $CD34^+$ cells enhances their capacity to repopulate nonobese diabetic/SCID mice in the short term and promotes erythroid differentiation (11). All these findings suggest that STAT5 is significantly active downstream in TPO signaling in HSCs. However, the role of STAT5 in LTR-HSCs remains uncharacterized.

Emerging evidence suggests that cancer stem cells sustain neoplasms. The idea of cancer stem cells is well established in acute myeloid leukemia and MPD (12, 13). Leukemic stem cells share self-renewal machineries, such as Bmi-1, with normal HSCs and constantly regenerate leukemic progeny with a limited proliferative and differentiation capacity (14, 15). One of the most recently recognized oncogenic signaling pathways involves the STAT proteins. Constitutive activation of STAT3 and STAT5 is frequently detected in a variety of tumor types (16). However, their contribution to cancer stem cell system is hitherto untested.

We characterized specific functions of STAT3 and STAT5 in LTR-HSCs by using their constitutively active forms of mutants and highly purified mouse HSCs. We clearly demonstrated that the activation of STAT5, but not STAT3, promotes HSC self-renewal and that STAT3 is dispensable for the maintenance of HSC in vivo. We further showed that sustained STAT5 activation in $CD34^-$KSL HSCs, but not in $CD34^+$c-$Kit^+$$Sca\text{-}1^+$ lineage marker$^-$ (KSL) progenitors, establishes MPD in mice, providing a good mouse model of leukemic hematopoiesis that helps understand a specific role for STAT5 in cancer stem cell systems.

RESULTS

STAT5 activation in HSCs

TPO promotes the self-renewal of LTR-HSCs in vitro (5, 6). Whether TPO induces STAT5 activation in purified HSCs has never been determined. $CD34^-$KSL cells represent only 0.004% of BM mononuclear cells and are highly enriched for LTR-HSCs (17). To visualize STAT5 activation in HSCs directly, we immunostained TPO-stimulated $CD34^-$KSL cells with an anti-phosho-STAT5A/B antibody (Fig. 1).

TPO stimulation induced high-level activation of STAT5A/B. Upon TPO stimulation, STAT5A/B became phosphorylated on tyrosine residues (Y694/Y699) and was localized to the euchromatic region of the nucleus that is devoid of DAPI staining. In contrast, IL-6 reportedly activates STAT3 and failed to support in vitro HSC self-renewal in our previous study (6). In fact, IL-6 stimulation of mouse M1 immature myeloid cells did not induce STAT5 activation at all (unpublished data). Unexpectedly, however, IL-6 induced STAT5 activation in $CD34^-$KSL cells. Nevertheless, the level of STAT5 activation was much weaker than that induced by TPO, and the vast majority of phosphorylated STAT5 stayed in the cytoplasm. Although the reason a substantial amount of phosphorylated STAT5 stays in the cytoplasm remains obscure, these data indicate a major role of STAT5 in TPO signaling in HSCs.

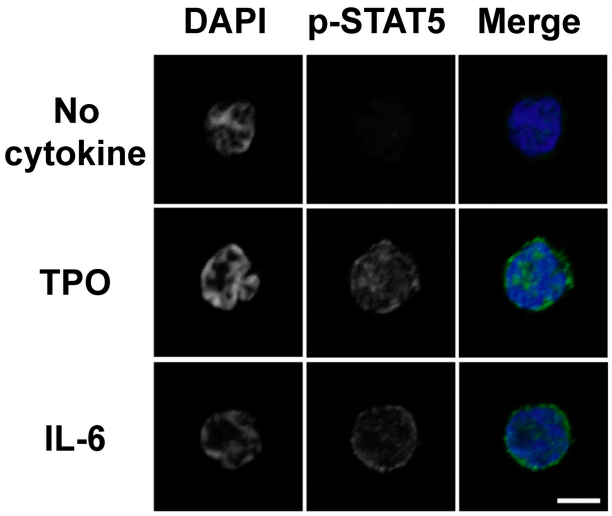

Figure 1. Immunodetection of STAT activation in $CD34^-$KSL cells. (A) $CD34^-$KSL cells were sorted in a culture medium drop supplemented with TPO or IL-6 on fibronectin-coated slide glasses. After 30 min of incubation at 37°C, STAT5 activation was assessed by immunocytological analysis using an anti-phospho-STAT5A/B. The localization of tyrosine-phosphorylated STAT5 was determined under a confocal microscope. Nuclear DAPI staining (blue; left) and immunofluorescent labeling of STAT5 (green; middle) are merged (right). Bar, 4 μm.

Characterization of constitutively active STAT3 and STAT5 mutants

To examine STAT5-specific functions in HSCs, we used retroviral constructs that express constitutively active STAT5A mutants. These constructs previously have been shown to mediate functions of STAT5A/B (Fig. 2 A and references 18, 19).

As a control, a retroviral construct that expresses constitutively active STAT3 mutant was also prepared (20). All mutants except for STAT3C could confer cytokine independence on a Ba/F3 IL-3–dependent pro-B cell line in a similar fashion (18, 19, and unpublished data). Among STAT5 mutants, however, STAT5 1*6 and STAT5 1*7 mutants could mediate high-level transcriptional activation of a STAT5 target gene, whereas STAT5 #2 was less effective (Fig. 2 B). Western blotting assessment showed comparable expression of each mutant in transduced cells (Fig. 2 B).

Selective activation of STAT5 supports multilineage differentiation of HSCs

$CD34^-$KSL cells are highly enriched for LTR-HSCs, of which ~60% can be defined as colony-forming units-neutrophil/

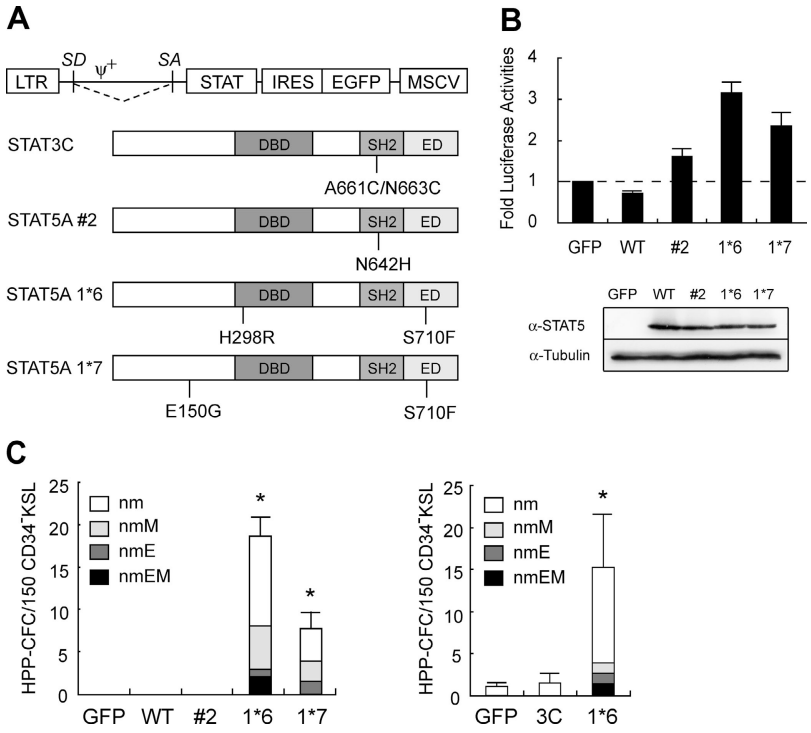

Figure 2. Selective activation of STAT5 supports multilineage differentiation of HSCs. (A) Schematic representation of the retroviral vector GCDNsam-IRES-EGFP harboring constitutively active *STAT3* and *STAT5A* mutant genes. Positions of point mutations are indicated. ψ^+, packaging signal; SD, splice donor; SA, splice acceptor; DBD, DNA binding domain; SH2, *src* homology domain 2; ED, effector domain. (B) Transcriptional activity and expression of STAT5A mutants. NIH 3T3 cells were cotransfected with 3x D1-SIE1-Luc luciferase reporter gene and pGCDNsam-IRES-EGFP (GFP), pGCDNsam-wild-type *STAT5A*-IRES-EGFP (WT), pGCDNsam-*STAT5A #2*-IRES-EGFP (#2), pGCDNsam-*STAT5A 1*6*-IRES-EGFP (1*6), or pGCDNsam-*STAT5A 1*7*-IRES-EGFP (1*7). The results are shown as the mean ± SD of triplicate cultures (top). Jurkat cells transduced with the indicated retroviruses were selected by cell sorting using GFP as a marker and then subjected to Western blot analysis using anti-mouse STAT5A and anti-α-tubulin antibodies (bottom). (C) Selective activation of STATs in HSCs. $CD34^-$KSL cells transduced with the indicated STAT5 mutants were subjected to colony assays in the presence of SCF only. The numbers of HPP-CFCs were retrospectively evaluated by counting colonies at d 10. Colonies derived from HPP-CFCs were recovered and examined for their composition with respect to CFCs. The results are shown as mean ± SD of triplicate cultures. *, statistically significant against GFP control (<0.01).

macrophage/Erythroblast/Megakaryocyte (CFU-nmEM), that exhibit multilineage differentiation capacity in vitro (4). To understand the role of STAT5 in proliferation and multilineage differentiation of HSCs, we first transduced $CD34^-$KSL cells with indicated *STAT5* mutant retroviruses. At 24 h after transduction, cells were subjected to the colony assay in the presence of stem cell factor (SCF) alone, a condition that does not support proliferation or multilineage differentiation of HSCs. In contrast to *GFP* control, $CD34^-$KSL cells expressing *STAT5 1*6* and *STAT5 1*7* retrovirus, but not *STAT5 #2* or wild-type *STAT5* retroviruses, gave rise to a significant number of high-proliferative-potential colonies (colony diameter >1 mm). Morphological analysis demonstrated that colonies generated from *STAT5 1*6*– or *STAT5 1*7*–expressing cells include nmEM colonies that consist of multilineage cells (Fig. 2 C). On the other hand, $CD34^-$KSL cells transduced with *STAT3C* generated only a few colonies of neutrophils and macrophages (Fig. 2 C). These data indicate that STAT5, but not STAT3, mainly mediates growth and differentiation signals in HSCs and their progeny.

Selective activation of STAT5 expands CFU-nmEM ex vivo

We next asked if STAT5 supports HSC self-renewal ex vivo. $CD34^-$KSL cells were transduced with each *STAT* mutant and were further incubated for 13 d (14-d ex vivo culture in total). In the presence of SCF and TPO, a condition that supports expansion of HSCs and progenitors rather than their differentiation, forced expression of wild-type and *STAT5* mutant gave no apparent growth advantage for the first 10 d compared with the *GFP* control (Fig. 3 A).

Notably, however, at day 7 of culture, *STAT5*-transduced cells contained numerous HPP-CFCs (Fig. 3 B). Morphological evaluation of the colonies revealed significant expansion of CFU-nmEM by both wild-type and STAT5 mutants. Given that 60% of freshly isolated $CD34^-$KSL cells can be defined as CFU-nmEM (4), a net expansion in CFU-nmEM by 10- (wild-type STAT5) to 20-fold (STAT5 1*6) occurred during 7-d culture (Fig. 3 C). Even when supplemented with SCF alone, cells expressing *STAT5 1*6* or *STAT5 1*7* showed mitotic activity that was significant, albeit weaker than that seen in the presence of SCF and TPO

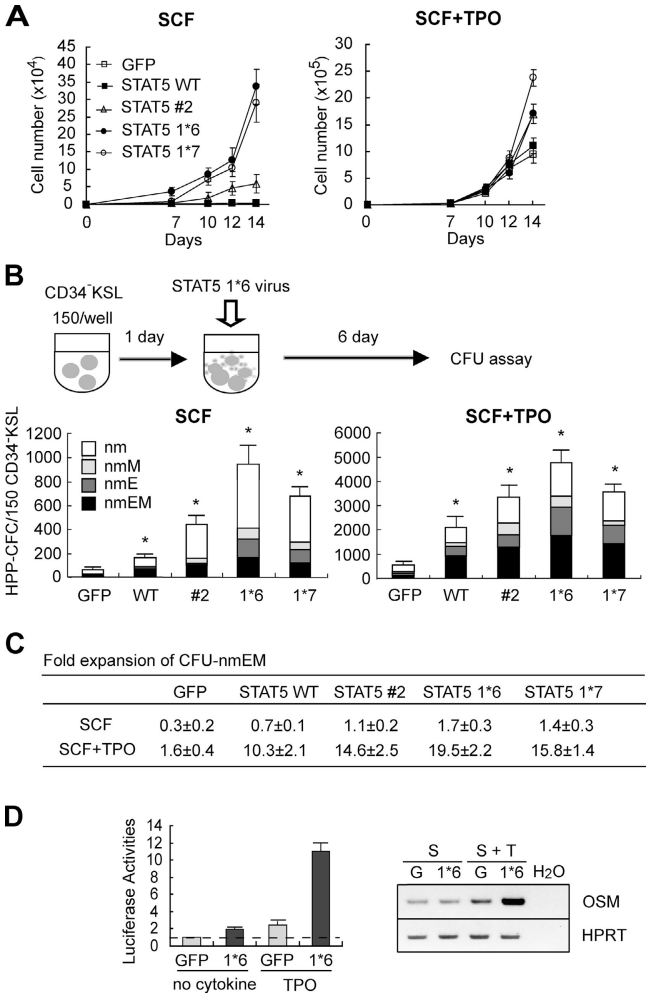

Fold expansion of CFU-nmEM	GFP	STAT5 WT	STAT5 #2	STAT5 1*6	STAT5 1*7
SCF	0.3±0.2	0.7±0.1	1.1±0.2	1.7±0.3	1.4±0.3
SCF+TPO	1.6±0.4	10.3±2.1	14.6±2.5	19.5±2.2	15.8±1.4

Figure 3. Ex vivo expansion of CFU-nmEM by selective activation of STAT5 in HSCs. (A) Growth of CD34$^-$KSL cells transduced with STAT5 mutants. CD34$^-$KSL cells transduced with the indicated retroviruses were cultured in the presence of SCF alone or of both SCF and TPO. The results are shown as mean ± SD of triplicate cultures. (B) Colony assays. At d 7 of culture, colony assays were performed to evaluate the content of HPP-CFC in culture. The colonies derived from HPP-CFCs were recovered and examined by microscopy to determine colony types. The results are shown as mean ± SD of triplicate cultures. *, statistically significant against GFP control (<0.02). (C) Net expansion of CFU-nmEM during the 7-d culture period. The results are shown as mean ± SD of triplicate cultures. (D) Synergistic effect of TPO and exogenous STAT5 1*6. 293 cells were cotransfected with ST5BS-luciferase reporter gene, pMY-human TPO receptor, and pGCDNsam-IRES-EGFP (GFP), or with pGCDNsam-*STAT5A 1*6*-IRES-EGFP (1*6), in the presence or absence of TPO (50 ng/ml). Fold luciferase activities are shown as the mean ± SD of triplicate cultures (left). CD34$^-$KSL cells transduced with pGCDNsam-IRES-EGFP (G) or pGCDNsam-*STAT5A 1*6*-IRES-EGFP (1*6) were cultured in the presence of SCF and TPO. At d 6, the cells were washed and resuspended in the medium containing SCF alone (S) or both SCF and TPO (S+T). After 24 h, cells were subjected to RT-PCR analysis on *OSM* gene expression (right). HPRT, hypoxanthine phosphoribosyltransferase.

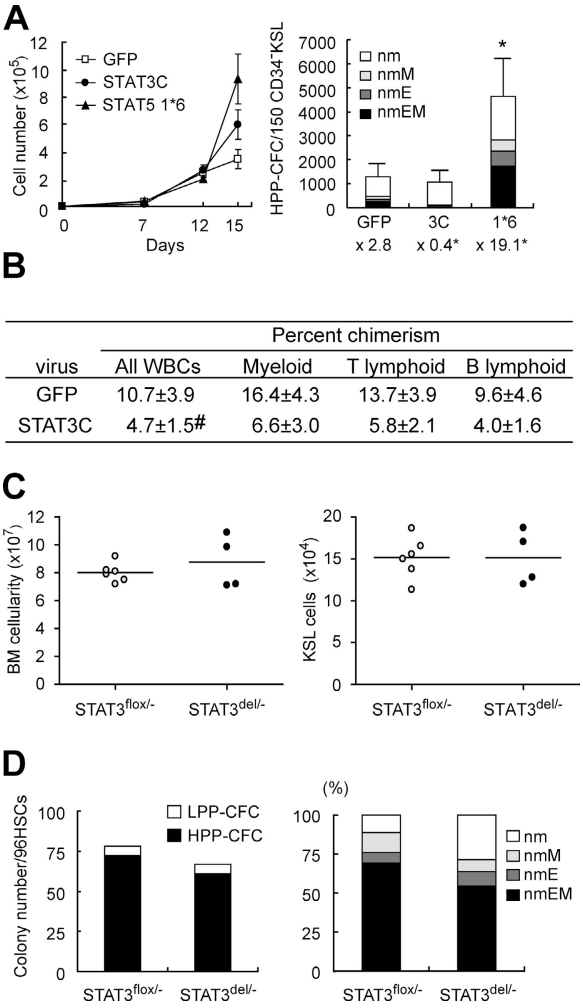

	Percent chimerism			
virus	All WBCs	Myeloid	T lymphoid	B lymphoid
GFP	10.7±3.9	16.4±4.3	13.7±3.9	9.6±4.6
STAT3C	4.7±1.5#	6.6±3.0	5.8±2.1	4.0±1.6

Figure 4. Role of STAT3 in HSCs. (A) Growth and the content of CFU-nmEM in culture of HSCs transduced with *STAT3C*. CD34$^-$KSL cells transduced with the indicated retroviruses were cultured in the presence of SCF and TPO, and their growth was monitored (left). At d 7 of culture, colony assays were performed to evaluate the content of HPP-CFC in culture (right). Expansion of CFU-nmEM is depicted on the bottom. The results are shown as mean ± SD of triplicate cultures. *, statistically significant against GFP control (<0.02). (B) Percent chimerism of donor cells in peripheral blood of recipients 12 wk after transplantation. CD34$^-$KSL cells transduced with indicated retroviruses were cultured in the presence of SCF and TPO. Competitive repopulation assays were performed using ex vivo cultured cells at d 7 corresponding to 30 initial CD34$^-$KSL cells per recipient mouse. The data are presented as mean ± SD ($n = 5$). #, statistically not significant; WBC, white blood cell. (C) Absolute numbers of BM cells and KSL cells in *STAT3$^{\Delta/-}$* mice 5 wk after conditional ablation of *STAT3*. The mean values are indicated as bars. (D) Growth and differentiation potential of *STAT3$^{\Delta/-}$* HSCs. 96 individual CD34$^-$KSL HSCs from *STAT3$^{flox/-}$* and *STAT3$^{\Delta/-}$* mice were sorted clonally into 96-well micro-titer plates in the presence of SCF, IL-3, TPO, and EPO. HPP-CFC and low-proliferative-potential colony-forming cell (LPP-CFC) numbers were evaluated retrospectively at d 14 (left). Colonies derived from HPP-CFC were examined for their composition with respect to colony-forming cells (right).

(Fig. 3 A). Although expression of *STAT5* did not expand CFU-nmEM under this stringent condition, it maintained the numbers of CFU-nmEM over 7-d culture (Fig. 3, B and C). To understand the molecular mechanism that explains a synergistic biological effect of TPO and exogenous STAT5 1*6 in HSCs, we compared their capacities to induce transcription of STAT5 target genes (Fig. 3 D). Both TPO stimulation and exogenous STAT5 1*6 expression presented moderate effects on transactivation of an artificial promoter as well as on an authentic STAT5 target gene, *Oncostatin M* (*OSM*). On the other hand, as expected, they showed a synergistic effect when combined with each other.

In contrast with STAT5, expression of *STAT3C* adversely affected the maintenance of multipotential progenitors. This adverse effect was manifest as a significantly decreased number of CFU-nmEM in culture and as somewhat promoted myeloid differentiation, although the LTR capacity of HSCs in vivo was not grossly affected (Fig. 4, A and B).

Alternately, expression of a dominant-negative STAT3 mutant (E434A/E435A), *STAT3D* (21) did not substantially affect the proliferation or multilineage differentiation potential of HSCs (unpublished data). To understand further the role of STAT3 in HSCs, we analyzed the effect of conditional ablation of the *STAT3* gene in HSCs. To establish mice with a conditional knockout of *STAT3* in hematopoietic cells, $STAT3^{flox/-}$ and *Mx1-Cre:*$STAT3^{flox/-}$ mice were injected with three doses of polyinocinic-polycytidylic acid (pIpC), and their BM was analyzed 5 wk later. Only a trace of STAT3 protein was detected in $STAT3^{\Delta/-}$ BM, and, importantly, phosphorylation of STAT3 was not detected at all upon treatment with granulocyte colony-stimulating factor (Fig. S1, available at http://www.jem.org/cgi/content/full/jem.20042541/DC1), indicating efficient Cre-mediated excision of the floxed *STAT3* gene in the BM.

The BM from $STAT3^{\Delta/-}$ mice and from controls contained similar numbers of cells in total and of hematopoietic stem and multipotential progenitor cells (KSL cells) (Fig. 4 C). Moreover, single-cell growth assays demonstrated that $STAT3^{\Delta/-}$ $CD34^-$KSL cells were able to form colonies at frequencies comparable with those of controls and retained multilineage differentiation potential (Fig. 4 D). These data correspond well with previous analyses showing no significant change in committed progenitor cell numbers in $STAT3^{\Delta/-}$ mice (22, 23) and indicate that the role of STAT3 in HSC is not essential.

To determine the mechanism whereby STAT5 activation induces CFU-nmEM expansion, we employed a paired-daughter cell assay to see if overexpression of *STAT5* mutants promotes symmetrical HSC division in vitro. After 24 h prestimulation, $CD34^-$KSL cells were transduced with a *STAT5 1*6* retrovirus for another 24 h. After transduction, single-cell cultures were initiated by micromanipulation. When a single cell underwent cell division, the daughter cells were separated again and were allowed to form colonies. To evaluate the commitment process of HSCs while excluding committed progenitors from this study, we selected daughter cells that were retrospectively inferred to have retained nmEM differentiation potential (4). Forced expression of *STAT5 1*6* unexpectedly did not change the frequency of symmetrical cell division of daughter cells (Fig. 5), indicating that STAT5 does not grossly influence intrinsic decisions determining cell fate.

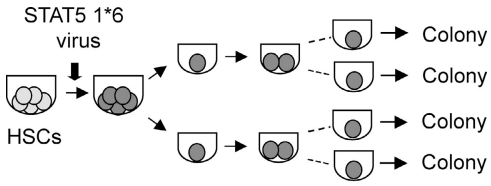

	expression vector	
Colony pair	GFP	STAT5 1*6
nmEM/nmEM	17 (45%)	19(53%)#
nmEM/nmE	3	1
nmEM/nmM	11	8
nmEM/nm	5	5
nmEM/m	2	3
Total	38	36

Figure 5. Effect of STAT5 on symmetrical cell division of HSCs. $CD34^-$KSL HSCs were transduced with either *GFP* or *STAT5 1*6* retroviruses. After 24 h of transduction, cells were separated clonally by micromanipulation. When a single cell underwent cell division, daughter cells were separated again by micromanipulation and were cultured further to permit full differentiation along myeloid lineages. The colonies were recovered for microscopy. Only the pairs whose parental cells were inferred to have retained neutrophil (n), macrophage (m), erythroblast (E), and Megakaryocyte (M) differentiation potential were selected. #, statistically not significant.

Selective activation of STAT5 maintains LTR-HSCs ex vivo and induces fatal MPD in vivo

To clarify whether LTR-HSCs were maintained in *STAT5* culture, we performed competitive repopulation assays using 7-d and 10-d ex vivo–cultured cells corresponding to 30 initial $CD34^-$KSL cells per recipient mouse. As previously reported (24), repopulation with cells expressing *STAT5 1*6* led to fatal MPD ~4 wk after transplantation (Fig. 6 A).

Mice receiving cells expressing *STAT5 1*7* mutant also developed MPD with a similar time course (Fig. 6 A). MPD induced by STAT5 was characterized by marked leukocytosis and splenomegaly. Histological analysis showed hypercellularity of the BM with increased numbers of maturing myeloid elements and effacement of the splenic white pulp caused by extramedullary hematopoiesis (unpublished data). As previously reported (24), STAT5-induced MPD accompanied a significant expansion of nontransduced cells as demonstrated by FACS analysis for GFP expression (Fig. 7 C and not depicted).

Although development of fatal MPD prohibited us from evaluating the LTR capacity of cells in *STAT5 1*6* and

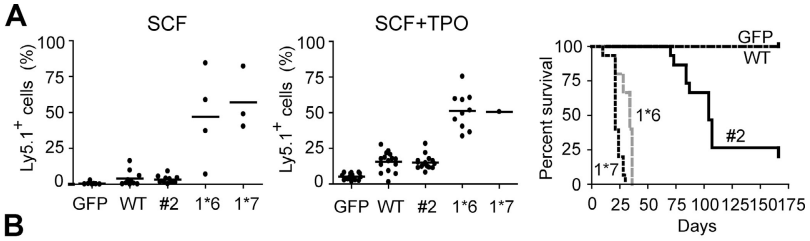

B

Cytokine	Culture days	Positive virus	Positive mice	Percent chimerism: All WBCs	Myeloid	T lymphoid	B lymphoid	RU
SCF	7	GFP	0/7	-	-	-	-	-
		WT	4/10	1.8±0.4	3.3±1.9	1.7±3.3	-	-
		#2	5/9	14.5±22.7	21.0±26.8	31.6±35.5	-	-
SCF+TPO	7	GFP	9/15	6.0±5.3	6.3±6.3	9.6±9.7	4.2±2.4	0.1±0.1
		WT	15/15	*16.4±12.6	25.6±14.1	25.8±18.5	13.2±11.7	0.5±0.5
		#2	10/10	*31.0±22.0	41.7±20.9	48.9±23.7	14.3±14.2	1.5±2.5
SCF+TPO	10	GFP	0/12	-	-	-	-	-
		WT	13/15	4.2±6.5	2.3±2.7	7.1±11.3	4.0±6.5	0.1±0.1
		#2	12/12	25.4±18.9	23.8±15.5	37.1±18.8	11.8±9.6	0.9±0.8

C

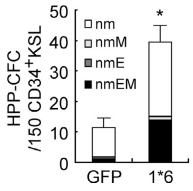

Transduced cell	CD34-KSL	CD34+KSL
WBC (x10^5/ml)	431.8 (65-1407)	42.5 (26-59)
Percent chimerism	51.1±12.9 (n=10)	0.08±0.05 (n=6)
Phenotype	MPD 15/15	MPD 0/6

Figure 6. Selective activation of STAT5 enhances repopulation activity of HSCs and induces MPD. (A) Percent chimerism of donor cells 4 wk after transplantation. CD34$^-$KSL cells were transduced with the indicated retroviruses and were further cultured in the presence of SCF alone or of both SCF and TPO. Competitive repopulation assays were performed using ex vivo cultured cells at d 7 corresponding to 30 initial CD34$^-$KSL cells per recipient mouse (SCF alone, $n = 10$; SCF+TPO, $n = 15$). Percent chimerism of donor cells in the peripheral blood of surviving recipients is plotted as dots, and mean values are indicated as bars (left and middle). Survival of recipient mice infused with cultured cells in the presence of SCF and TPO was monitored and is shown as Kaplan-Meier plots (right). (B) Percent chimerism of donor cells in the peripheral blood of recipients 12 wk after transplantation. The data are expressed as mean ± SD. Recipient mice with chimerism>1% in all white blood cells (WBC) were judged to be reconstituted (positive mice). *, statistically significant against GFP control (<0.01). Myeloid, T-lymphoid, and B-lymphoid represent Gr-1$^+$ and/or Mac-1$^+$, CD4$^+$ or CD8$^+$, and B220$^+$ cells, respectively. (C) STAT5 targets CD34$^-$KSL HSCs in the development of MPD. CD34$^+$KSL multipotential progenitor cells as well as CD34$^-$KSL HSCs were transduced with *STAT5 1*6* and, 24 h after the initiation of transduction, cells were subjected to colony assays in the presence of SCF, TPO, IL-3, and EPO. Numbers of HPP-CFC and of each CFC type were evaluated at d 14 (left). *, statistically significant against GFP control (<0.01). 6 d after the initiation of transduction, cells corresponding to 30 initial CD34$^-$KSL cells or 150 initial CD34$^+$KSL cells were injected into lethally irradiated recipient mice along with competitor cells. The peripheral blood data 4 wk after transplantation are presented (right).

*STAT5 1*7* ex vivo culture, mice reconstituted with cells transduced with wild-type *STAT5* did not develop MPD at all, and a significant percentage of mice with *STAT5 #2*–transduced cells survived more than 3 mo after transplantation, although most of them developed fatal MPD in the end (Fig. 6 A). Of note, 12 wk after transplantation, HSCs transduced with either wild-type *STAT5* or *STAT5 #2* showed significantly higher repopulation than did the *GFP* control (Fig. 6 B). The capacity of wild-type STAT5 or STAT5 #2 to maintain LTR-HSCs was prominent in 10-d ex vivo culture, in which no LTR activity was detected for the GFP control (Fig. 6 B). The repopulating potential in a cell population can be quantitated by calculating repopulation units (RU) from the chimerism of donor cells and the number of competitor cells. HSCs transduced with wild-type *STAT5* or *STAT5 #2* manifested fivefold and 15-fold higher RU, respectively, compared with GFP controls when cultured for 7 d ex vivo (Fig. 6 B). We next performed competitive repopulation assays using 7-d ex vivo–cultured cells in the presence of SCF alone. As expected from the capacity of STAT5 to maintain CFU-nmEM ex vivo under this stringent condition, HSCs transduced with either wild-type *STAT5* or *STAT5 #2* established long-term repopulation, although they somehow failed to contribute to B lymphopoiesis (Fig. 6 B). Moreover, mice infused with HSCs that expressed *STAT5 1*6* or *STAT5 1*7* when maintained with SCF alone developed fatal MPD, as had mice infused with cells cultured in the presence of SCF and TPO (Fig. 6 A and unpublished survival data).

Leukemic stem cells could be derived from either HSCs or from more restricted progenitors that have reacquired the stem cell capability for self-renewal (13, 15, 25, 26). To uncover the role of constitutive activation of STAT5 in MPD development directly, we next transduced CD34$^+$KSL mul-

tipotential progenitor cells with *STAT5 1*6*. Selective activation of STAT5 in CD34$^+$KSL cells also promoted their proliferation and multilineage differentiation (Fig. 6 C). Notably, however, CD34$^+$KSL cells transduced with *STAT5 1*6* failed entirely to repopulate BM and did not contribute to MPD development (Fig. 6 C). Moreover, transduction of *STAT5 1*6* did not enhance the serial replating capacity of CD34$^+$KSL progenitor cells in vitro (Fig. S2, available at http://www.jem.org/cgi/content/full/jem.20042541/DC1).

These data indicate that activation of STAT5 alone does not confer self-renewal capacity on committed progenitors or the ability to induce and to maintain MPD. Conversely, only HSCs originally retaining LTR capacity could induce MPD in vivo when transduced with *STAT5 1*6*. According to this evidence, we performed modified HSC measurement, i.e., measurement of MPD-initiating cell numbers in *STAT5 1*6* ex vivo cultures. Using limiting dilution transplantation analysis, the frequency of MPD-initiating cells in the 10-d ex vivo culture was defined as 1 of 10 initial CD34$^-$KSL cells at the observation time point of 2 mo (Fig. S3 A, available at http://www.jem.org/cgi/content/full/jem.20042541/DC1).

At day 10 of ex vivo culture, the *GFP* control culture contained no LTR-HSCs (Fig. 6 B). Given that transduction efficiency was ~75% in this experiment, and that one of three initial CD34$^-$KSL cells exhibits LTR activity in vivo (17), at least 4 of 10 initial LTR-HSCs were maintained in the *STAT5 1*6* culture. These data correspond well with results of clonality analyses of MPD, which demonstrated at least three- to five-clone oligoclonality (Fig. S3 B). Longer observation might note some increase in the frequency of LTR-HSCs as inferred from the high-level contribution of the donor cells in surviving mice at 2 mo (Fig. S3 A).

OSM is not principally responsible for MPD development induced by STAT5

OSM has been reported as a STAT5 target gene responsible for the development of MPD induced by TEL/JAK2 (24). In our RT-PCR analyses of STAT5 target gene expression, *OSM* expression was significantly increased in HSCs transduced with active-form STAT5 mutants (Fig. 7 A). To analyze the role of *OSM* in the development of MPD induced by selective activation of STAT5, we transduced CD34$^-$KSL cells from *OSM*$^{-/-}$ and *OSM receptor (OSMR)*$^{-/-}$ mice with *STAT5 1*6*, then transplanted them into lethally irradiated mice. In mice infused with either *OSM*$^{-/-}$ or *OSMR*$^{-/-}$ HSCs transduced with *STAT5 1*6*, MPD developed as when wild-type HSCs were infused (Fig. 7 B), and expansion of nontransduced cells was still observed (Fig. 7 C), indicating that *OSM* is not the STAT5 target gene principally involved in the development of MPD.

DISCUSSION

In this study, we directly showed that TPO activates STAT5 in HSCs (Fig. 1). Interestingly, IL-6, which failed to maintain

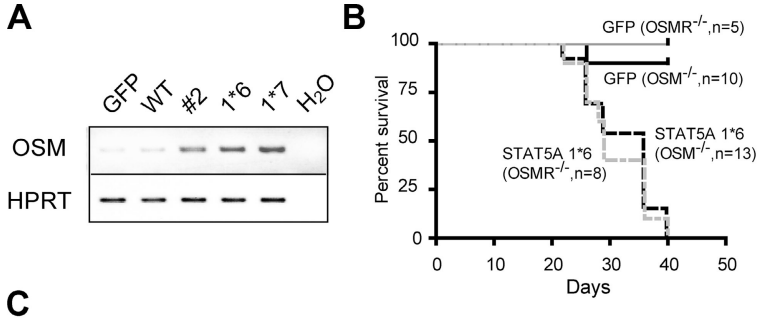

C

virus	Mouse no.	WBC (x10^2/μl)	myeloid cells (%)	GFP$^+$ cells in myeloid cells (%)
GFP	n=9	47.3 (26-72)	70.5 (64.8-78.5)	42.2 (20.7-55.7)
STAT5 1*6	1	59	80.9	14.5
	2	239	75.1	74.5*
	3	447	78.9	94.1
	4	506	88.4	71.8*
	5	175	68.5	78.1*
	6	319	67.9	64.7*
	7	190	74.1	59.8*
	Average	276.4 (59-506)	76.2 (67.9-88.4)	65.3 (14.5-94.1)

Figure 7. Oncostatin M signal is unnecessary for STAT5-induced MPD. (A) RT-PCR analysis of *OSM* gene expression in transduced HSCs. CD34$^-$KSL cells transduced with the indicated retroviruses were cultured in the presence of SCF and TPO. At d 7 of culture, cells were subjected to RT-PCR. HPRT, hypoxanthine phosphoribosyltransferase. (B) Development of MPD with *STAT5 1*6*-transduced *OSM*$^{-/-}$ and *OSMR*$^{-/-}$ HSCs. CD34$^-$KSL cells from *OSM*$^{-/-}$ or *OSMR*$^{-/-}$ HSCs were transduced with *STAT5 1*6* and were further cultured in the presence of SCF and TPO. Competitive repopulation assays were performed using ex vivo cultured cells at d 7 corresponding to 30 initial CD34$^-$KSL cells per recipient mouse. Kaplan-Meier plots of survival are presented. (C) Peripheral blood data 4 wk after transplantation of *OSM*$^{-/-}$ HSCs are presented. Note that a significant percentage of Gr-1$^+$ and/or Mac-1$^+$ myeloid cells in MPD mice does not express GFP (identified by asterisk).

HSC self-renewal in vivo in our previous study (6), did not effectively induce STAT5 activation. These data support the notion that STAT5 contributes to the self-renewal of HSCs.

Loss-of-function analyses involving STAT5 have demonstrated its critical role in hematopoiesis. *STAT5A/STAT5B* double-mutant mice (*STAT5AB*$^{-/-}$) exhibit multilineage peripheral blood cytopenias, BM progenitor-cell reduction, and a profound impairment of repopulation potential in competitive BM transplantation assays (8, 9). Although the number of HSCs is not significantly changed in *STAT5A/B*$^{-/-}$ mice, a defect in *STAT5A/B*$^{-/-}$ HSC self-renewal was uncovered by serial transplantation experiments in which *STAT5A/B*$^{-/-}$ HSCs failed to provide consistent engraftment in tertiary hosts (27). These hematopoietic defects in *STAT5A/B*$^{-/-}$ mice, except for peripheral blood cell counts, cannot be rescued by *bcl-2* expression, indicating that STAT5 plays an essential role in the maintenance and expansion of self-renewing HSCs and progenitors (28). The role of STAT5 in HSC self-renewal was demonstrated clearly by gain-of-function analyses in this study. Expression of constitutively active *STAT5* mutants expanded multipotential progenitors (Fig. 3) and promoted self-renewal of HSCs (Fig. 6). During 7-d ex vivo culture, a net 20-fold CFU-nmEM expansion and 15-fold higher repopulation activity were obtained in *STAT5* mutant cultures (Figs. 3 and 6). Of note, expression of *STAT5* mutants substantially slowed loss of LTR-HSCs through successive cell divisions during 10-d ex vivo culture (Fig. S3 A). Although expression of *STAT5* mutants did not lead to an apparent HSC expansion, this result could be explained in part by the finding that it does not grossly affect the frequency of symmetrical cell division of CD34^{-}KSL HSCs in vitro (Fig. 5). In this regard, the role of STAT5 in HSC self-renewal contrasts sharply with that of Bmi-1, an essential regulator of HSC self-renewal that promotes symmetrical cell division of HSC in paired daughter-cell assays (4). However, the effect of STAT5 activation is comparable to that of HoxB4 and of Bmi-1. Like these HSC regulators, STAT5 could be a novel target for therapeutic manipulation of HSCs.

Notably, transduction of *STAT5* mutants into CD34^{-}KSL HSCs supported their proliferation and multilineage differentiation in the presence of SCF alone and allowed CD34^{-}KSL HSCs to give rise to significant numbers of high-proliferative-potential colonies, including nmEM colonies (Fig. 2 C). This observation directly supports a major role for STAT5 as a downstream signaling molecule of early-acting and lineage-restricted late-acting cytokines. Nevertheless, the combination of exogenous *STAT5* mutants with TPO exhibited synergistic effects on HSCs as well as on the transcription of STAT5 target genes (Figs. 3 and 6). These findings indicate that other downstream signals activated by TPO, including mitogen-activated protein kinase and phosphatidylinositol 3-kinase pathways might function synergistically with activated STAT5. Such signals or pathways also might play a role in full activation of STAT5 through, for example, its phosphorylation. In contrast to our data, STAT5 recently has been demonstrated to promote erythroid differentiation preferentially when expressed in human CD34^{+} cells (11). We also observed erythropoietin-independent erythroblast expansion when we transduced human CD34^{+} cells with *STAT5 1*6* (unpublished data). However, in CD34^{-}KSL HSCs or CD34^{+}KSL progenitor cells, *STAT5 1*6* expression did not promote expansion of erythroid-committed progenitor cells or erythroid differentiation in vitro. Nor did it enhance their self-renewal capacity in vitro (Figs. S2 and S4, available at http://www.jem.org/cgi/content/full/jem.20042541/DC1).

These data suggest that the different effects of *STAT5 1*6* in human and mouse are caused by a difference in species rather than by a difference in target cells. Alternatively, different in vitro culture conditions, i.e., with or without stromal cells, might have affected the results.

In contrast to STAT5, STAT3 is activated efficiently by signals mediated by gp130. Specific activation of gp130 by a combination of IL-6 and soluble IL-6 receptor has been demonstrated to expand human CD34^{+} nonobese diabetic/SCID-mouse repopulating cells ex vivo (29). This finding suggests the participation of STAT3 in HSCs. However, recent conditional gene-ablation analysis in hematopoietic cells uncovered the specific role of STAT3 in negative regulation of granulopoiesis by inducing expression of a signaling inhibitor, *SOCS3* (22, 30). In this study, we further demonstrated that STAT3 is not necessary for the maintenance of HSCs in vivo or for the full unfolding in vitro of the capacity of HSCs for proliferation and differentiation (Fig. 4, C and D). On the other hand, selective activation of STAT3 counteracted TPO signaling with respect to expansion of CFU-nmEM in vitro; instead, it committed HSCs to myeloid differentiation (Fig. 4 A). These findings correlate well with those in neural precursor cells in which STAT3 plays a major role in the commitment toward astrocyte lineage (31). Although expression of a dominant-negative STAT3 reportedly impairs the long-term hematopoietic repopulation capacity of HSCs (32), this finding should be interpreted carefully because dominant-negative forms of STAT3 potentially inhibit the activity not only of STAT3 but also of STAT1, a heterodimer partner for STAT3 (31). We previously reported that IL-6 enhances mitogenic activity of CD34^{-}KSL cells but cannot maintain self-renewing HSCs in vitro (6). This finding might be explained by an adverse effect of STAT3 on HSC self-renewal.

Constitutive activation of STAT3 and STAT5 is detected frequently in a variety of tumor types (16). Constitutive activation of STAT5 often is observed in myeloid leukemias of both acute and chronic types, whereas activation of STAT3 is observed in lymphoid tumors. STAT5 signaling has been shown to promote oncogenesis. In chronic myelogenous leukemia, STAT5 is activated persistently by the BCR-ABL kinase, and in acute leukemia, it is activated persistently by the FLT3 receptor tyrosine kinase with constitutively activating internal tandem duplication (16). Of note, constitutive STAT5 activation has been demonstrated to be

essential in a mouse model of MPD induced by TEL-JAK2 fusion protein (24). MPD is a group of disorders characterized by cellular proliferation of one or more hematopoietic cell lineages distinct from acute leukemia. Chronic MPD consists of four diseases, including polycythemia rubra vera, primary thrombocythemia, agnogenic myeloid metaplasia, and chronic myelogenous leukemia. Some evidence indicates that MPDs are clonal diseases that arise from malignant transformation of a single stem cell. In this study, we clearly demonstrated that STAT5 targets $CD34^-KSL$ HSCs, but not $CD34^+KSL$ progenitor cells, to induce MPD. Selective activation of STAT5 in $CD34^+KSL$ cells promoted their proliferation and multilineage differentiation. Importantly, however, expression of *STAT5 1*6* in $CD34^+KSL$ cells did not enhance their in vitro self-renewal capacity (Fig. S2) and failed to establish repopulation of hematopoiesis in vivo (Fig. 6 C). These data indicate that although STAT5 contributes to progenitor expansion and to progenitor differentiation, it does not confer LTR capacity on $CD34^+KSL$ progenitors. They also indicate that the ability of STAT5 to promote HSC self-renewal is most crucial in establishment of a leukemic stem cell system. In this regard, the role of STAT5 in a leukemic stem cell system is quite different from the roles of *MOZ-TIF2* and *MLL-ENL* oncogenes, which confer properties of leukemic stem cells on committed hematopoietic progenitors (25, 26). In our previous study, other self-renewal regulators such as HoxB4 and Bmi-1also failed to confer LTR capacity on $CD34^+KSL$ progenitor cells (4). These findings indicate that self-renewal is tightly regulated in a multifactorial fashion.

The mechanism whereby STAT5 regulates HSC self-renewal remains to be defined. In these experiments, the biological effect of each STAT5 mutant, including CFU-nmEM expansion, enhancement of HSC self-renewal ex vivo, and the severity of MPD in vivo (Figs. 3 C and 6, A and B) correlated well with each mutant's transactivation activity (Figs. 2 B and 7 A). For example, STAT5 1*6 and STAT5 1*7 induced severe MPD, whereas wild-type STAT5 did not induce MPD at all. These observations indicate that certain STAT5 targets actually are responsible for the HSC self-renewal process. Several genes have been shown to be regulated by STAT5, including *cyclin D1* (33), *p21*, *c-fos*, *Id-1*, *pim-1*, *Bcl-X_L*, *CIS*, and *OSM*. Among them, *cyclin D1* is preferentially expressed in primitive hematopoietic cells (Iwama et al., unpublished data); *cyclin $D1^{-/-}D2^{-/-}D3^{-/-}$* mice exhibit a profound defect in the expansion of hematopoietic stem and progenitor cells (34). Recent findings in *Bmi-1*–, *ATM*-, and *JunB*-deficient mice underscore the impact of G_1-S regulation by $p16^{INK4a}$ and $p19^{ARF}$ in HSC self-renewal (4, 13, 35). *Cyclin D1* could be one of the candidate genes through which STAT5 could regulate this process. Detailed expression profiling of STAT5-regulated genes in HSCs would help us understand further the molecular mechanisms underlying HSC self-renewal.

As previously reported (24), STAT5-induced MPD accompanied a significant expansion of nontransduced cells (unpublished data). The cell nonautonomous contribution to the disease phenotype indicates involvement of growth factors in a paracrine fashion. Dysregulation of several cytokines, including TGF-β, platelet-derived growth factor, and insulinlike growth factor-1, in fact is implicated in the pathogenesis of MPD in humans (36). In a mouse model of TEL/JAK2-induced MPD, *OSM* has been implicated as one of the direct STAT5 targets responsible for cell nonautonomous phenotype (24). However, the ablation of neither *OSM* nor *OSMR* from HSCs had any gross effect on the development of STAT5-induced MPD, including cell nonautonomous phenotype (Fig. 7). We have previously reported that STAT5 activation promotes *IL-6* gene transcription in a NF-κB–dependent manner (37). It will be intriguing to pursue hitherto unidentified STAT5 targets that contribute to the MPD phenotype in a paracrine fashion.

Selective activation of STAT5 in HSCs unveiled the specific role of STAT5 in normal HSCs as well as in leukemic stem cells in a mouse model of MPD. STAT5 activation was tightly involved in the development and maintenance of abnormal hematopoiesis of myeloid lineage. Further investigations of the role of STAT5 in normal and leukemic stem cells should provide novel insights into the molecular mechanisms that regulate cancer stem cell systems.

MATERIALS AND METHODS

Mice. *$Stat3^{flox/-}$* mice were generated by mating *$STAT3^{flox}$* mice, in which the DNA base pairs encoding the tyrosine phosphorylation site in Stat3 are flanked by two loxP sites (*$STAT3^{flox/flox}$*)(38), with *$STAT3^{+/-}$* mice, in which exons 20–22 are replaced by a neomycin resistance gene in the knockout allele (39). To establish mice with a conditional knockout of *STAT3* in hematopoietic cells, *$STAT3^{flox/-}$* mice were mated with mice from a transgenic line bearing Cre recombinase driven by the IFN-inducible *Mx1* promoter (40). Expression of Cre was induced by injecting mice intraperitoneally with 250 μg of pIpC (Sigma-Aldrich) three times at 2-d intervals, as previously described (40). 4-wk-old *$STAT3^{flox/-}$* mice and *Mx1-Cre:$STAT3^{flox/-}$* mice were injected with pIpC and analyzed 5 wk later. *$OSM^{-/-}$* mice and *$OSMR^{-/-}$* mice (41) were backcrossed at least eight times onto a C57BL/6 (B6-Ly5.2) background. All experiments using mice received approval from the Tokyo University Administrative Panel for the Animal Care.

Purification of mouse HSCs. Mouse HSCs ($CD34^-KSL$ cells) were purified from BM cells of 2-mo-old mice. In brief, low-density cells were isolated on Lymphoprep (1.086 g/ml; Nycomed). The cells were stained with an antibody cocktail consisting of biotinylated anti–Gr-1, –Mac-1, -B220, -CD4, -CD8 and –Ter-119 monoclonal antibodies (BD Biosciences). Lineage-positive cells were depleted with streptavidin-coupled magnetic beads (M-280; Dynal). The remaining cells were stained further with FITC-conjugated anti-CD34, PE-conjugated anti–Sca-1, and allophycocyanin-conjugated anti–c-Kit antibodies (BD Biosciences). Biotinylated antibodies were detected with streptavidin-Texas red (Invitrogen). Four-color analysis and sorting were performed on a FACSVantage SE System (Becton Dickinson).

Retroviral constructs and cDNAs. Constitutively active forms of mouse *STAT3* and *STAT5* (*STAT3C*, *STAT5A*, *STAT5A #2*, *STAT5A 1*6,* and *STAT5A 1*7*) have been described (18–20). Murine wild-type *STAT5A*, *STAT5A #2*, *STAT5A 1*6*, *STAT5A 1*7*, and *STAT3C* cDNAs were subcloned into a site upstream of an *IRES-EGFP* construct in pGCDNsam, a retroviral vector with an LTR derived from murine stem cell virus (4).

Transduction of mouse $CD34^-KSL$ cells. Recombinant retroviruses were produced as previously described (4). $CD34^-KSL$ were deposited into

96-well micro-titer plates coated with recombinant fibronectin fragment (Takara Shuzo, Co., Ltd.) at 150 cells/well and were incubated in α-MEM supplemented with 1% FBS, 100 ng/ml mouse SCF, and 100 ng/ml human TPO (PeproTech) for 24 h. The cells were transduced with a retrovirus vector at a multiplicity of infection of 600 in the presence of protamine sulfate (10 μg/ml; Sigma-Aldrich) and recombinant fibronectin fragment (1 μg /ml) for 24 h. After transduction, cells were further incubated in S-Clone SF-O3 (Sanko Junyaku Co. Ltd.) supplemented with 1% FBS and either 20 ng/ml SCF only or with 20 ng/ml SCF plus 50 ng/ml TPO and were subjected to assays at the indicated time point. $CD34^+$KSL were cultured in the presence of 100 ng/ml of SCF, human TPO, and human IL-6 and were transduced similarly. In all experiments, transduction efficiency was ~80% as judged by GFP expression.

Colony assays. $CD34^-$KSL cells transduced with indicated retroviruses were plated in methylcellulose medium (StemCell Technologies Inc.) supplemented with 50 ng/ml mouse SCF only or with 50 ng/ml mouse SCF, 20 ng/ml mouse IL-3, 50 ng/ml human TPO, and 2 units/ml human erythropoietin (EPO; PeproTech). The culture dishes were incubated at 37°C in a 5% CO_2 atmosphere. GFP^+ colony numbers were counted at d 14. Colonies derived from HPP-CFCs (colony diameter >1 mm) were recovered, cytospun onto glass slides, then subjected to May-Gruenwald-Giemsa staining for microscopy.

Paired-daughter cell assays. $CD34^-$KSL cells were transduced with indicated retroviruses as described above. After 24 h of transduction, micromanipulation techniques were used to separate cells clonally into 96-well microtiter plates in S-Clone SF-O3 supplemented with 0.1% BSA, 50 ng/ml SCF, and 50 ng/ml TPO, as previously described (4). When a single cell underwent cell division and gave rise to two daughter cells, daughter cells were again separated into different wells by micromanipulation. Individual paired daughter cells were further incubated in S-Clone SF-O3 supplemented with 10% FBS, 20 ng/ml SCF, 50 ng/ml TPO, 20 ng/ml IL-3, and 5 unit/ml EPO. The colonies generated from each daughter cell were recovered for microscopy.

Competitive repopulation assays. Competitive repopulation assays were performed using the Ly5 congenic mouse system. In brief, hematopoietic cells from B6-ly5.2 mice were mixed with BM competitor cells (B6-Ly5.1) and were transplanted into B6-ly5.1 mice irradiated at a dose of 9.5 Gy. In the case of Ly5.1 hematopoietic cells, cells were mixed with BM competitor cells (B6-Ly5.2) and were transplanted into B6-ly5.2 mice. After transplantation, peripheral blood of recipients was stained with biotinylated anti-Ly5.2 and PE-conjugated anti-Ly5.1 (BD Biosciences). Cells then were stained with either a mixture of allophycocyanin-conjugated anti-Mac-1 and anti-Gr-1 antibodies or a mixture of PE-conjugated anti-CD4 and anti-CD8 antibodies and PE-Cy7-conjugated anti-B220 antibody (BD Biosciences). RU were calculated using Harrison's method as follows: RU = (percent donor cells) × (number of competitor cells) × 10^{-5}/100 − (percent donor cells). By definition, each RU represents the repopulating activity of 10^5 BM cells. In this study, the number of BM competitors was fixed as 2×10^5 cells. The test cell/competitor cell ratio defined above was applied to Harrison's formula as follows: RU = T/C ratio × 2 (4).

Detection of phosphorylated STAT5 in $CD34^-$KSL cells. $CD34^-$KSL cells were sorted in a serum-free culture medium drop supplemented with 0.1% BSA and either 100 ng/ml TPO or 100 ng/ml IL-6 on fibronectin-coated slide glasses. The sorted cells were incubated at 37°C for 30 min. After fixation with 2% paraformaldehyde and blocking in 10% goat serum for 1 h at room temperature, cells were incubated with a primary antibody, anti-phospho-STAT5A/B, clone 8–5-2 (Upstate Biotechnology) at a dilution of 1:500 for 12 h at 4°C. The cells then were washed and were incubated with Alexa Fluor 488 goat anti-mouse secondary antibody (Invitrogen) at a dilution of 1:500 for 30 min at room temperature. Immunofluorescence was observed with a Leica TCS SP2 AOBS confocal microscope.

RT-PCR. Semiquantitative RT-PCR was performed using normalized cDNA by quantitative PCR using TaqMan rodent GAPDH control reagent (PerkinElmer), as described (4). Primer sequences are available from the authors on request.

Luciferase assays. NIH 3T3 cells (5×10^4 cells) were seeded in a 24-well plate and cultured for 24 h. Cells were then transfected with 200 ng of indicated expression vector along with 100 ng of a reporter gene containing either trimerized wild-type or mutated STAT5 binding sites from the *cyclin D1* promoter (3× D1-SIE1-Luc and 3× D1-SIE1m-Luc, respectively) (33) and 600 pg of pRL-CMV, an expression vector of *Renilla luciferase*, using Lipofectamine Plus reagent (Invitrogen). At 24 h after transfection, the cells were deprived of serum for 12 h and then subjected to luciferase assays using the Dual-luciferase Reporter System (Promega). Relative firefly luciferase activities were calculated by normalizing transfection efficiency to *Renilla luciferase* activities. 293 cells were cotransfected with the ST5BS-Luc luciferase reporter gene (42), pMY-human TPO receptor, and either pGCDNsam-IRES-EGFP or pGCDNsam-*STAT5A 1*6*-IRES-EGFP in the presence or absence of TPO (50 ng/ml), then similarly processed.

Western blotting. Jurkat cells transduced with the indicated retroviruses were selected by cell sorting for GFP expression, and subjected to Western blot analysis using anti–mouse STAT5 (L-20; Santa Cruz Biotechnology, Inc.) and anti-α-tubulin (Ab-1; Oncogene Science) antibodies.

Online supplemental material. Fig. S1 provides data for Cre-mediated excision of STAT3. Fig. S2 provides data for serial replating capacity of $CD34^-$KSL HSCs and $CD34^+$KSL progenitor cells transduced with *STAT5 1*6*. Fig. S3 provides the MPD-initiating cell numbers in the *STAT5 1*6* ex vivo culture and the clonality of *STAT5 1*6*–induced MPD. Fig. S4 provides data for effect of *STAT5 1*6* expression on erythroid commitment and erythroid progenitor expansion. Online supplemental material is available at http://www.jem.org/cgi/content/full/jem.20042541/DC1.

We thank Drs. T. Hirano and T. Matsumura, M. Onodera, H. Nakajima, J.E. Darnell, and U. Lichtenberg for providing *STAT3D* cDNA, 3xD1-SIE-Luc, pGCDNsam-IRES-EGFP, ST5BS-Luc, *STAT3C* cDNA, and *Mx-Cre* mice, respectively; Y. Morita (ReproCELL Inc.) for excellent technical assistance; and Dr. A. Knisely for critical reading of the text.

This work was supported in part by grants from the Ministry of Education, Culture, Sport, Science and Technology, Japan.

The authors have no conflicting financial interests.

Submitted: 14 December 2004
Accepted: 26 May 2005

REFERENCES

1. Levy, D.E., and J.E. Darnell. 2002. STATs: transcriptional control and biological impact. *Nat. Rev. Mol. Cell Biol.* 3:651–662.
2. Mui, A.L., H. Wakao, A.M. O'Farrell, N. Harada, and A. Miyajima. 1995. Interleukin-3, granulocyte-macrophage colony stimulating factor and interleukin-5 transduce signals through two STAT5 homologs. *EMBO J.* 14:1166–1175.
3. Antonchuk, J., G. Sauvageau, and R.K. Humphries. 2002. HOXB4-induced expansion of adult hematopoietic stem cells ex vivo. *Cell.* 109:39–45.
4. Iwama, A., H. Oguro, M. Negishi, Y. Kato, Y. Morita, H. Tsukui, H. Ema, T. Kamijo, Y. Katoh-Fukui, H. Koseki, et al. 2004. Enhanced self-renewal of hematopoietic stem cells mediated by the polycomb gene product, Bmi-1. *Immunity.* 21:843–851.
5. Yagi, M., K.A. Ritchie, E. Sitnicka, C. Storey, G.J. Roth, and S. Bartelmez. 1999. Sustained ex vivo expansion of hematopoietic stem cells mediated by thrombopoietin. *Proc. Natl. Acad. Sci. USA.* 96:8126–8131.
6. Ema, H., H. Takano, K. Sudo, and H. Nakauchi. 2000. In vitro self-renewal division of hematopoietic stem cells. *J. Exp. Med.* 192:1281–1288.
7. Kimura, S., A.W. Roberts, D. Metcalf, and W.S. Alexander. 1998. Hematopoietic stem cell deficiencies in mice lacking c-Mpl, the recep-

tor for thrombopoietin. *Proc. Natl. Acad. Sci. USA*. 95:1195–1200.
8. Snow, J.W., N. Abraham, M.C. Ma, N.W. Abbey, B. Herndier, and M.A. Goldsmith. 2002. STAT5 promotes multilineage hematolymphoid development in vivo through effects on early hematopoietic progenitor cells. *Blood*. 99:95–101.
9. Bunting, K.D., H.L. Bradley, T.S. Hawley, R. Moriggi, B.P. Sorrentino, and J.N. Ihle. 2002. Reduced lymphomyeloid repopulating activity from adult bone marrow and fetal liver of mice lacking expression of STAT5. *Blood*. 99:479–487.
10. Kyba, M., R.C.R. Perlingeiro, R.R. Hoover, C.W. Lu, J. Pierce, and G.Q. Daley. 2003. Enhanced hematopoietic differentiation of embryonic stem cells conditionally expressing Stat5. *Proc. Natl. Acad. Sci. USA*. 100:11904–11910.
11. Schuringa, J.J., K.Y. Chung, G. Morrine, and M.A.S. Moore. 2004. Constitutive activation of STAT5A promotes human hematopoietic stem cell self-renewal and erythroid differentiation. *J. Exp. Med*. 200: 623–635.
12. Hope, K.J., L. Jin, and J.E. Dick. 2004. Acute myeloid leukemia originates from a hierarchy of leukemic stem cell classes that differ in self-renewal capacity. *Nat. Immunol*. 5:738–743.
13. Passegue, E., E.F. Wagner, and I.L. Weissman. 2004. JunB deficiency leads to a myeloproliferative disorder arising from hematopoietic stem cells. *Cell*. 119:431–443.
14. Lessard, J., and G. Sauvageau. 2003. Bmi-1 determines proliferative capacity of normal and leukemic stem cells. *Nature*. 423:255–260.
15. Passegue, E., C.H. Jamieson, L.E. Ailles, and I.L. Weissman. 2003. Normal and leukemic hematopoiesis: are leukemias a stem cell disorder or a reacquisition of stem cell characteristics? *Proc. Natl. Acad. Sci. USA*. 100(Suppl 1):11842–11849.
16. Yu, H., and R. Jove. 2004. The STATs of cancer–new molecular targets come of age. *Nat. Rev. Cancer*. 4:97–105.
17. Osawa, M., K.-I. Hanada, H. Hamada, and H. Nakauchi. 1996. Long-term lymphohematopoietic reconstitution by a single CD34-low/negative hematopoietic stem cells. *Science*. 273:242–245.
18. Onishi, M., T. Nosaka, K. Misawa, A.L. Mui, D. Gorman, M. McMahon, A. Miyajima, and T. Kitamura. 1998. Identification and characterization of a constitutively active STAT5 mutant that promotes cell proliferation. *Mol. Cell. Biol*. 18:3871–3879.
19. Yamada, K., K. Ariyoshi, M. Onishi, A. Miyajima, F. Hayakawa, M. Towatari, H. Saito, Y. Oka, S. Asano, T. Nosaka, and T. Kitamura. 2000. Constitutively active STAT5A and STAT5B in vitro and in vivo: mutation of STAT5 is not a frequent cause of leukemogenesis. *Int. J. Hematol*. 71:46–54.
20. Bromberg, J.F., M.H. Wrzeszczynska, G. Devgan, Y. Zhao, R.G. Pestell, C. Albanese, and J.E. Darnell Jr. 1999. Stat3 as an oncogene. *Cell*. 98:295–303.
21. Nakajima, K., Y. Yamanaka, K. Nakae, H. Kojima, M. Ichiba, N. Kiuchi, T. Kitaoka, T. Fukuda, M/ Hibi, and T. Hirano. 1996. A central role for Stat3 in IL-6-induced regulation of growth and differentiation of M1 leukemia cells. *EMBO J*. 15:3651–3658.
22. Lee, C.K., R. Raz, R. Gimeno, R. Gertner, B. Wistinghausen, K. Takeshita, R.A. DePinho, and D.E. Levy. 2002. STAT3 is a negative regulator of granulopoiesis but is not required for G-CSF-dependent differentiation. *Immunity*. 17:63–72.
23. Kamezaki, K., K. Shimoda, A. Numata, T. Haro, H. Kakumitsu, M. Yoshie, M. Yamamoto, K. Takeda, T. Matsuda, S. Akira, et al. 2005. The roles of Stat3 and ERK in G-CSF signaling. *Stem Cells*. 23:252–263.
24. Schwaller, J., E. Parganas, D. Wang, D. Cain, J.C. Aster, I.R. Williams, C.-K. Lee, R. Gerthner, T. Kitamura, J. Frantsve, et al. 2000. Stat5 is essential for the myelo- and lymphoproliferative disease induced by TEL/JAK2. *Mol. Cell*. 6:693–704.
25. Huntly, B.J., H. Shigematsu, K. Deguchi, B.H. Lee, S. Mizuno, N. Duclos, R. Rowan, S. Amaral, D. Curley, I.R. Williams, et al. 2004. MOZ-TIF2, but not BCR-ABL, confers properties of leukemic stem cells to committed murine hematopoietic progenitors. *Cancer Cell*. 6:587–596.
26. Cozzio, A., E. Passegue, P.M. Ayton, H. Karsunky, M.L. Cleary, and I.L. Weissman. 2003. Similar MLL-associated leukemias arising from self-renewing stem cells and short-lived myeloid progenitors. *Genes Dev*. 17:3029–3035.
27. Bradley, H.L., C. Couldrey, and K.D. Bunting. 2004. Hematopoietic-repopulating defects from STAT5-deficient bone marrow are not fully accounted for by loss of thrombopoietin responsiveness. *Blood*. 103: 2965–2972.
28. Snow, J.W., N. Abraham, M.C. Ma, S.K. Bronson, and M.A. Goldsmith. 2003. Transgenic bcl-2 is not sufficient to rescue all hematolymphoid defects in STAT5A/B-deficient mice. *Exp. Hematol*. 31: 1253–1258.
29. Ueda, T., K. Tsuji, H. Yoshino, Y. Ebihara, H. Yagasaki, H. Hisakawa, T. Mitsui, A. Manabe, R. Tanaka, K. Kobayashi, et al. 2000. Expansion of human NOD/SCID-repopulating cells by stem cell factor, Flk2/Flk3 ligand, thrombopoietin, IL-6, and soluble IL-6 receptor. *J. Clin. Invest*. 105:1013–1021.
30. Croker, B.A., D. Metcalf, L. Robb, W. Wei, S. Mifsud, L. DiRago, L.A. Cluse, K.D. Sutherland, L. Hartley, E. Williams, et al. 2004. SOCS3 is a critical physiological negative regulator of G-CSF signaling and emergency granulopoiesis. *Immunity*. 20:153–165.
31. Bonni, A., Y. Sun, M. Nadal-Vicens, A. Bhatt, D.A. Frank, I. Rozovsky, N. Stahl, G.D. Yancopoulos, and M.E. Greenberg. 1997. Regulation of gliogenesis in the central nervous system by the JAK-STAT signaling pathway. *Science*. 278:477–483.
32. Oh, I.H., and C.J. Eaves. 2002. Overexpression of a dominant negative form of STAT3 selectively impairs hematopoietic stem cell activity. *Oncogene*. 21:4778–4787.
33. Matsumura, I., T. Kitamura, H. Wakao, H. Tanaka, K. Hashimoto, C. Albanese, J. Downward, R.G. Pestell, and Y. Kanakura. 1999. Transcriptional regulation of the cyclin D1 promoter by STAT5: its involvement in cytokine-dependent growth of hematopoietic cells. *EMBO J*. 18:1367–1377.
34. Kozar, K., M.A. Ciemerych, V.I. Rebel, H. Shigematsu, A. Zagozdzon, E. Sicinska, Y. Geng, Q. Yu, S. Bhattacharya, R.T. Bronson, et al. 2004. Mouse development and cell proliferation in the absence of D-cyclins. *Cell*. 118:477–491.
35. Ito, K., A. Hirao, S. Matsuoka, K. Takubo, I. Hamaguchi, K. Nomiyama, K. Hosokawa, K. Sakurada, N. Nakagata, Y. Ikeda, et al. 2004. Regulation of oxidative stress by ATM is required for self-renewal of hematopoietic stem cells. *Nature*. 431:997–1002.
36. Doll, D.C., N.Y. Gabrail, and A.F. List. 1995. Introduction: myeloproliferative disorders. *Semin. Oncol*. 22:305–306.
37. Kawashima, T., K. Murata, S. Akira, Y. Tonozuka, Y. Minoshima, S. Feng, H. Kumagai, H. Tsuruga, Y. Ikeda, S. Asano, et al. 2001. STAT5 induces macrophage differentiation of M1 leukemia cells through activation of IL-6 production mediated by NF-kappaB p65. *J. Immunol*. 167:3652–3660.
38. Takeda, K., T. Kaisho, N. Yoshida, J. Takeda, T. Kishimoto, and S. Akira. 1998. Stat3 activation is responsible for IL-6-dependent T cell proliferation through preventing apoptosis: generation and characterization of T cell-specific Stat3-deficient mice. *J. Immunol*. 161:4652–4660.
39. Takeda, K., K. Noguchi, W. Shi, T. Tanaka, M. Matsumoto, N. Yoshida, T. Kishimoto, and S. Akira. 1997. Targeting disruption of the mouse Stat3 gene leads to early embryonic lethality. *Proc. Natl. Acad. Sci. USA*. 94:3801–3804.
40. Kuhn, R., F. Schwenk, M. Aguet, and K. Rajewsky. 1995. Inducible gene targeting in mice. *Science*. 269:1427–1429.
41. Tanaka, M., Y. Hirabayashi, T. Sekiguchi, T. Inoue, M. Katsuki, and A. Miyajima. 2003. Targeted disruption of oncostatin M receptor results in altered hematopoiesis. *Blood*. 102:3154–3162.
42. Nakajima, H., P.K. Brindle, M. Handa, and J.N. Ihle. 2001. Functional interaction of STAT5 and nuclear receptor co-repressor SMRT: implications in negative regulation of STAT5-dependent transcription. *EMBO J*. 20:6836–6844.